Restoration of High-Renewable-Penetrated Distribution Systems Considering Uncertain Repair Workloads

Xiaotian Sun, *Student Member, IEEE,* Haipeng Xie, *Member, IEEE,* Zhaohong Bie, *Senior Member, IEEE,* and Gengfeng Li, *Member, IEEE*

***Abstract*—In distribution systems with high penetration of renewable energy, the fast restoration after extreme events faces a variety of uncertainties from the output of distributed renewable generations as well as the incomplete knowledge on accurate repair workloads of fault components. Considering these uncertainties, the paper proposes an implicit decision rule based restoration-oriented combined unit-crew dispatch (RCUCD) method to boost the ex-post restoration. First, a "wait and see" uncertainty model is presented to depict the nonanticipativity of repair workloads of fault components. Thereby, a dynamic crew grouping dispatch algorithm is proposed to dispose the uncertainties in repair workloads based on the improved time-space network theory. Further, a multi-stage stochastic RCUCD model is set up for post-disaster restoration. Based on implicit decision rules, the proposed model is reformulated into a mixed integer linear programming (MILP) problem by introducing axillary safety region variables. To boost the computational efficiency, the simplified RCUCD model as well as the rolling look-ahead RCUCD model is proposed. The effectiveness and efficiency of the proposed methods are tested on IEEE 34-bus and 69-bus distribution systems.**

***Index Terms*—Implicit decision rule, nonanticipativity, renewable energy, repair crew, restoration.**

NOMENCLATURE

Sets and Indices

$\mathcal{S}$, s	Set and index of scenarios.
$\hat{\mathcal{S}}$, $\hat{s}$	Set and index of all-scenario-feasible scenarios.
$\mathcal{H}$, h	Set and index of fault components.
$\mathcal{B}$, b	Set and index of buses in the distribution system.
$\mathcal{L}$, l	Set and index of transmission lines in the distribution system.
$\mathcal{G}$, g	Set and index of distributed generation units in the distribution system.
$\mathcal{R}$, r	Set and index of renewable energy generations in the distribution system.
$\mathcal{D}$, d	Set and index of loads in the distribution system.
$\mathcal{E}$, e	Set and index of energy storages in the distribution system.
$\mathcal{C}$, c	Set and index of repair crews.
Π_i^+/Π_i^-	Set of transmission lines start/end at bus i.
Ω	Set of arcs in the time-space network.
Ω_m^+/Ω_m^-	Set of arcs start/terminate at location m.
$\mathcal{N}$, m, u	Set and indices of nodes in the time-space network.
t	Index of time interval.

Deterministic Parameters

α_s	Weighting factor of scenarios.
$\alpha_{\hat{s}}$	Weighting factor of all-scenario-feasible scenarios.
ΔT	Length of dispatch interval.
r_l/x_l	Resistance/reactance of line l.
$\underline{P}_g^G/\overline{P}_g^G$	Lower/upper active power output limit of distributed generator.
$\underline{Q}_g^G/\overline{Q}_g^G$	Lower/upper reactive power output limit of distributed generator.
$\overline{P}_e^{ES,ch}$	Maximum energy storage charging active power.
P_d^D/Q_d^d	Original active/reactive load consumption.
$\overline{P}_e^{ES,dch}$	Maximum energy storage discharging active power.
$\underline{E}_e/\overline{E}_e$	Lower/upper capacity bound of energy storage.
η_e^{ch}/η_e^{dch}	Efficiency of energy storage charging/discharging.
NR	Number of staffs in all repair crews.

Uncertain Parameters

W_h	Uncertain workload of fault component h.
P_r^{RE}	Uncertain potential maximum active power output of renewable power generation r.

Variables

$H_{l,t,s}/G_{l,t,s}$	Active/reactive power flow on line l.
$P_{r,t,s}^{acc}/Q_{r,t,s}^{acc}$	Active/reactive power of accommodated renewable energy.
$P_{g,t,s}^G/P_{g,t,s}^G$	Active/reactive power of distributed generation unit.
$P_{d,t,s}^R/Q_{d,t,s}^R$	Active/reactive power of restored load consumption.
$P_{e,t,s}^{ES}$	Active power of energy storage output.
$V_{i,t,s}/V_{j,t,s}$	Bus voltage at the start/end of line l.
$u_{l,t,s}$	Binary variable representing status of line l.
$\delta_{c,(m,u)}^t$	Arc of repair crew c from location m to u.
$n_{c,(m,u)}^t$	Number of staffs in crew c from location m to u.

Other symbols are defined as required in the main text.

This paper was supported by the Science and Technology Project of State Grid Co., Ltd (SGJX0000KXJS900322).

X. Sun, H. Xie, Z. Bie and G. Li are with the State Key Laboratory of Electrical Insulation and Power Equipment, Xi'an Jiaotong University, Xi'an, China, 710049. (e-mail:haipengxie@mail.xjtu.edu.cn).

I. Introduction

A. Background and Motivation

TOWARDS the climate crisis, a growing number of countries have made commitment to reach carbon neutral by mid-21^{st}-century or soon after [1]. To achieve this goal, the renewable energy penetration in power systems will witness a new round of growth. The distributed generation, expected as a significant means to utilize the renewable energy, will further reform urban distribution systems. From the view of resilience towards high-impact-low-probability (HILP) events, the high penetration of renewable energy will provide more resources to recover [2]. However, renewable energy, e.g. wind power and photovoltaic, bring uncertainties to the power balance, especially for islanding after HILP events. Also, the distribution systems themselves face uncertainties from the stochastic repair workloads after HILP events, resulting in inscrutable crew dispatch for optimal recovery. Therefore, uncertainties pose a significant challenge to the promotion of resilience for urban distribution systems with a high penetration of renewable energy.

To dispose the adversity of uncertainties in ex-post restoration, nonanticipativity [3], [4] and all-scenario-feasibility [5] should be considered. In power system dispatch, nonanticipativity requires that the dispatch decision of the current dispatch interval should only depend on the realized uncertainties of previous intervals [6], [7]. Moreover, as the name states, all-scenario-feasibility means that the dispatch scheme decided in the previous dispatch intervals should be a feasible solution to all possible scenarios in the realization of uncertainties of upcoming dispatch intervals [8]–[10]. Nonanticipativity is closely related to all-scenario-feasibility and supplement each other. Considering that the distributed renewable energy generations formulate the major fraction of electric power sources in modern urban distribution systems, the utilization of renewable energy generation has a more prominent importance. Without the consideration of nonanticipativity and all-scenario-feasibility, renewable energy utilization of conventional restoration-oriented dispatch methods is restricted by the ramping constraints. This will directly result in the potential loss in electric energy sources, which is in adverse to the fast and economic restoration of distribution systems. Therefore, the restoration-oriented dispatch in the distribution system with high penetration of renewable energy requires nonanticipativity and all-scenario-feasibility of dispatch decisions.

Moreover, the uncertainties of repair workloads for fault components also affects the restoration process. The impact of uncertain repair workloads of fault components to repair crew dispatch and distribution system function recovery need to be addressed. Additionally, the repair crews need to be adjusted according to the repair workloads, while currently this has been neglected in research.

Therefore, this paper focuses on the restoration of distribution systems with high penetration of renewable energy, considering uncertainties from both distributed renewable energy generation and infrastructure repairs.

B. Literature Review

The resilience performance of power systems under an extreme weather can be technically divided into five stages, namely pre-disturbance resilient state, disturbance progress, post-disturbance degraded state, restoration progress and post-restoration state [10]–[12]. As one of the most effective way to enhance the power system resilience, restoration strategies have been extensively studied in the literature [13]–[18], but few of them consider the contribution of renewable energy generations in the restoration. In [19], resilience metrics for both long term planning and short-term operation of renewable integrated distribution system is formulated. Start-up of generation units, renewable energy generation and device availability assessment were considered in [20], and a power system restoration solution was provided. An adaptive model predictive control based strategy is proposed in [21] to coordinate the renewable penetrated distribution system restoration and distributed energy resources operation. It should be noted that the expected power generation of renewable resources is used in [14], [16], [21]. Thus, it is not applicable to the high renewable penetrated distribution systems. In the case with high renewable penetration level, the uncertainties in the process of distribution system restoration is unable to be omitted, otherwise the operation safety would be endangered.

Considering the fluctuant and intermittent generation of renewable energy resources, stochastic [19], [20] and robust [15], [22] based optimization methods are commonly adopted. By Monte Carlo simulation, a scenario based stochastic programming model is constructed in [19], [20]. Dispatch and evaluation are based on the stochastic programming model. However, considering that the continuity of renewable energy outputs, dispatch decisions on finite scenarios are not able to prove the feasibility of infinite possible realizations. In [15], [22], a tri-level min-max-min structure based robust optimization model is set up, while the result is not applicable for extreme ramping scenarios [4]. It was proved in [4], [23] that both stochastic and robust based optimization are not able to provide an all-scenario-feasible solution while considering the nonanticipativity of renewable energy generation. To make it clear, the high penetration level of renewable energy demands a more reliable and conservative dispatch scheme, especially in the post-disaster period. Thus, a novel unit commitment method is required. Implicit decision rule based method [24], which is a novel proposed unit commitment and economic dispatch method, is able to provide an all-scenario-feasible solution with nonanticipativity by extracting a few extreme scenarios. Moreover, considering the impaired connectivity and the gradually recovered transmission lines in post-disaster period, a more severe challenge on power balance is proposed for the distribution system operator [4], [22]–[25].

The recovery of power system function is based on the maintenance of power system infrastructure [11]. An efficient dispatch plan of limited repair crews is able to boost the length of restoration process and enhance the resilience of the distribution system. In [13], [24], repair crew dispatch is separated into a two-stage optimization problem. The fault components are clustered to different depots to release the

computational burden, and then the routes of repair crews are determined by each depot. In [16], a universal routing model for operation, repair and energization agents is proposed. The model is able to formulate an energization path for restoration process. However, repair crews are dispatched according to the deterministic repair time in the aforementioned research. Uncertain repair time of fault components are considered in [26]. The lognormal distributed repair time together with the uncertainty of load demand is dealt by progressive hedging algorithm.

Overall, the utilization of renewable energy generation in restoration-oriented dispatch of the distribution system with high penetration of renewable energy is still a gap to fill, while the detailed modeling of uncertainties in repair work is also a novel topic at the same time.

C. Contributions and Paper Organization

Considering the aforementioned background and literature review, this paper proposes a combined unit and repair crew dispatch model for the fast restoration of distribution systems with a high renewable energy penetration level. The nonanticipativity of renewable energy generation and repair workloads of fault components are captured and disposed in the proposed model. The model is reformulated into a mixed integer linear programming (MILP) problem based on implicit decision rule method. Comparisons of the proposed model and the deterministic model are carried out in case studies.

The contributions of this paper are threefold:

1) modeling the nonanticipativity for repair workloads in a "wait and see" model. The uncertain range information is obtained initially, whereas the actual repair workload in need is achieved only if a repair crew reach the location and complete a fast detection.

2) proposing a dynamic crew grouping model of routing and grouping decisions of repair crews to dispose the nonanticipativity of repair workloads. The time-space network modeling method is extended with the repair crew grouping constraints.

3) formulating the restoration-oriented combined unit-crew dispatch (RCUCD) model with the respect to nonanticipativity of renewable energy generations and repair workloads, then reformulating it into a MILP problem based on the implicit decision rule.

The reminder of the paper is organized as follows. Section II states the assumptions in uncertain repair time model. Section III describes the restoration-oriented combined unit-crew dispatch (RCUCD) model. Section IV presents the implicit decision rule based formulation of the proposed model and its simplification. Section V and VI are the case study and the conclusion, respectively.

II. Modeling Assumptions of Uncertain Repair Workloads

As aforementioned, this paper focuses on the restoration process out of the whole process under extreme weather. The restoration progress can be compartmentalized into two successive phases [26], namely the damage assessment phase and the repair implementation phase. Fault identification algorithms, data from preserved sensors, reports from terminal customers and unmanned aerial vehicle patrol after the end of the extreme weather are able to perform the damage assessment. Then, the repair implementation phase starts. In this phase, with the knowledge of component damage information, the depots assign repair crews under a certain dispatch scheme.

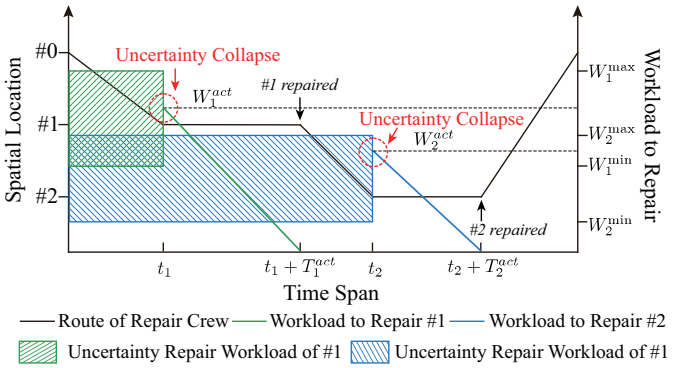

Fig. 1. Illustration of nonanticipative repair workloads and their realization.

The common assumptions of the restoration progress are: (i) the restoration starts at the closure of the extreme weather; (ii) the depot is aware of the knowledge of the fault components. Note that in assumption (ii), previous research on routing repair crews utilizes the location information and repair time information. However, in most cases the repair workloads and their corresponding repair times are difficult to achieve, named as *the nonanticipativity of repair workloads*. It is more realistic that the ranges of uncertain repair workloads are received in damage assessment phase while the actual repair workload of each fault component cannot be obtained until a repair crew reaches its location and implements a quick detection. The time of quick detection is neglected in this paper because it is negligible when compared to repair times. This is named as the "wait and see" characteristic of the uncertainty of the repair workload.

In this way, the repair workload of each fault component is a random variable with a known interval and its value is determined after the detection by the repair crew, as shown in Fig. 1. #0, #1 and #2 represents the spatial location of depot, fault component 1 and fault component 2, respectively. The repair crew starts from the depot, executes repair tasks of component 1 and component 2 successively, and finally returns to the depot. In the perspective of repair crew, the decision-making process is presented below.

$t = 0$: With known workload intervals $[W_1^{\min}, W_1^{\max}]$ and $[W_2^{\min}, W_2^{\max}]$, the repair crew decided to execute the maintenance of fault component 1 first.

$t \in (0, t_1)$: The repair crew moving towards location #1.

$t = t_1$: After a fast detection, the repair workload of fault component 1, W_1^{act}, is obtained.

$t \in (t_1, t_1 + T_1^{act})$: The repair crew was working on the maintenance of fault component 1.

$t = t_1 + T_1^{act}$: Component 1 was repaired. The repair crew decided to execute the maintenance of fault component 2.

$t \in (t_1 + T_1^{act}, t_2)$: The repair crew moving to location #2.

$t = t_2$: After a fast detection, the repair workload of fault component 1, W_2^{act}, is obtained.

$t \in (t_2, t_2 + T_2^{act})$: The repair crew was working on the maintenance of fault component 2.

$t = t_2 + T_2^{act}$: Component 2 was repaired. The repair crew decided to go back to the depot.

It is clear that at the time when routing decision is made, the actual repair workload and repair time required for component 1 and 2 have not been obtained, and the only information is the uncertainty interval of the repair workload of the two components. The uncertainties of repair workload of fault components are modeled via the box uncertainty set as shown in (1). Note that the box uncertainty set is mentioned here for the sake of simplicity, and irregular uncertainty sets, e.g., with budget constraints to describe the severity of the extreme weather, are also available for the method proposed in this paper.

$$\mathcal{W} = \{W_{h,s} | W_h^{\min} \le W_{h,s} \le W_h^{\max}; h \in \mathcal{H}, \forall s \in \mathcal{S}\} \quad (1)$$

where $\mathcal{W}$ is the uncertainty set of the workloads to repair the fault components; $W_h^{\min}$ and $W_h^{\max}$ denote the minimum and maximum workload for the maintenance of component h; $W_{h,s}$ is the realization of repair workloads in scenario s.

Take component 1 as example, the uncertain repair workload W_1 is collapsed to its actual value W_1^{act} at time t. The same collapse of uncertainty also occurs in component 2 at t_2. It has critical impact on not only the dispatch of repair crews but also the operation of power system in restoration process, especially when the nonanticipativity of repair workload is combined with the nonanticipativity of renewable energy generation.

III. Mathematical Formulation

A. Modeling of Distribution System Operation

The linearized Distflow model [27] is widely used and verified in distribution system resilience related research. The equations of Distflow model are formulated as below.

1) System-wide Constraints:

$$\sum_{l \in \Pi_i^+} H_{l,t,s} - \sum_{l \in \Pi_i^-} H_{l,t,s} = A_{r,i}^R P_{r,t,s}^{acc} + A_{g,i}^G P_{g,t,s}^G + A_{e,i}^{ES} P_{e,t,s}^{ES} - A_{d,i}^D P_{d,t,s}^R \quad \forall i \in \mathcal{B}, \forall s \in \mathcal{S}, \forall t \quad (2)$$

$$\sum_{l \in \Pi_i^+} G_{l,t,s} - \sum_{l \in \Pi_i^-} G_{l,t,s} = A_{r,i}^R Q_{r,t,s}^{acc} + A_{g,i}^G Q_{g,t,s}^G - A_{d,i}^D Q_{d,t,s}^R \quad \forall i \in \mathcal{B}, \forall s \in \mathcal{S}, \forall t \quad (3)$$

$$(u_{l,t,s} - 1)M \le V_{i,t,s} - V_{j,t,s} - (r_l H_{l,t,s} + x_l G_{l,t,s}) \le (1 - u_{l,t,s})M \quad \forall l \in \mathcal{L}, \forall s \in \mathcal{S}, \forall t \quad (4)$$

$$1 - \epsilon \le V_{i,t,s} \le 1 + \epsilon \quad \forall i \in \mathcal{B}, \forall s \in \mathcal{S}, \forall t \quad (5)$$

where $A_{r,i}^R$, $A_{g,i}^G$, $A_{e,i}^{ES}$ and $A_{d,i}^D$ are connection matrix of renewable energy generations, distributed generations, energy storages and loads respectively. Constraints (2)-(5) are system-wide constraints for the distribution system, of which constraints (2) and (3) are nodal active and reactive power balance constraints; constraint (4) is the power flow constraint of each line in the distribution system, where big-M method is adopted to model the line outage status; constraint (5) denotes the acceptable voltage fluctuation in restoration process, and the tolerance interval ϵ is set as 5%.

2) Individual Constraints:

$$0 \le P_{r,t,s}^{acc} \le P_{r,t,s}^{RE} \quad \forall r \in \mathcal{R}, \forall s \in \mathcal{S}, \forall t \quad (6)$$

$$-Q_{r,t,s}^{RE} \le Q_{r,t,s}^{acc} \le Q_{r,t,s}^{RE} \quad \forall r \in \mathcal{R}, \forall s \in \mathcal{S}, \forall t \quad (7)$$

$$\mathcal{X} = \{P_{r,t,s}^{RE} | P_{r,t}^{RE,\min} \le P_{r,t,s}^{RE} \le P_{r,t}^{RE,\max}; r \in \mathcal{R}, \forall s \in \mathcal{S}, \forall t\} \quad (8)$$

where $P_{r,t,s}^{RE}$ is the maximum renewable power generation; $Q_{r,t,s}^{RE}$ denotes the reactive power output limitation of the inverter; $P_{r,t}^{RE,\max}$ and $P_{r,t}^{RE,\min}$ represent the upper and lower limit of the uncertain interval of renewable energy generation, respectively; $\mathcal{X}$ is the uncertainty set. Constraint (6)-(7) are accommodated renewable energy generation constraints. The box uncertainty set of renewable energy generation is modelled by constraint (8). Note that polyhedron uncertainty sets are also applicable in the proposed method. Herein we adopt the box uncertainty set for the sake of simplicity.

$$0 \le P_{d,t,s}^R \le P_d^D \quad \forall d \in \mathcal{D}, \forall s \in \mathcal{S}, \forall t \quad (9)$$

$$Q_{d,t,s}^R = P_{d,t,s}^R \tan(\cos^{-1} \varphi_d) \quad \forall d \in \mathcal{D}, \forall s \in \mathcal{S}, \forall t \quad (10)$$

where φ_d denotes the power factor of load d. Constraints (9)-(10) are the restored load constraints, where the restored active and reactive load should be in the same proportion as the original load at the bus.

$$\underline{P}_g^G \le P_{g,t,s}^G \le \overline{P}_g^G \quad \forall g \in \mathcal{G}, \forall s \in \mathcal{S}, \forall t \quad (11)$$

$$\underline{Q}_g^G \le Q_{g,t,s}^G \le \overline{Q}_g^G \quad \forall g \in \mathcal{G}, \forall s \in \mathcal{S}, \forall t \quad (12)$$

$$-\Delta_g^P \le P_{g,t,s}^G - P_{g,t-1,s}^G \le \Delta_g^P \quad \forall g \in \mathcal{G}, \forall s \in \mathcal{S}, \forall t \quad (13)$$

$$-\Delta_g^Q \le Q_{g,t,s}^G - Q_{g,t-1,s}^G \le \Delta_g^Q \quad \forall g \in \mathcal{G}, \forall s \in \mathcal{S}, \forall t \quad (14)$$

where constraints (11)-(14) are individual constraints for distributed generation units in the distribution system, of which (11)-(12) are active and reactive power output constraints, respectively; constraints (13)-(14) are ramping constraints of the distributed generation units. It should be noted that ramp-rate constraints of distributed generation units are critical in high renewable penetrated distribution systems [28]–[30]. To restore maximum loads in the post-disaster period, renewable energy generations are in crucial position, thus maximum accommodated renewable energy generation is in expectation, which enforce the flexibility of the distributed generation units to be the binding constraints. Therefore, they are worth to be taken into consideration.

$$-\overline{P}_e^{ES,ch} \le P_{e,t,s}^{ES} \le \overline{P}_e^{ES,ch} \quad \forall e \in \mathcal{E}, \forall s \in \mathcal{S}, \forall t \quad (15)$$

$$\underline{E}_e \le E_{e,ini} - \sum_{v=1}^{t} f_e(P_{e,v,s}^{ES}) \le \overline{E}_e \quad \forall e \in \mathcal{E}, \forall s \in \mathcal{S}, \forall t \quad (16)$$

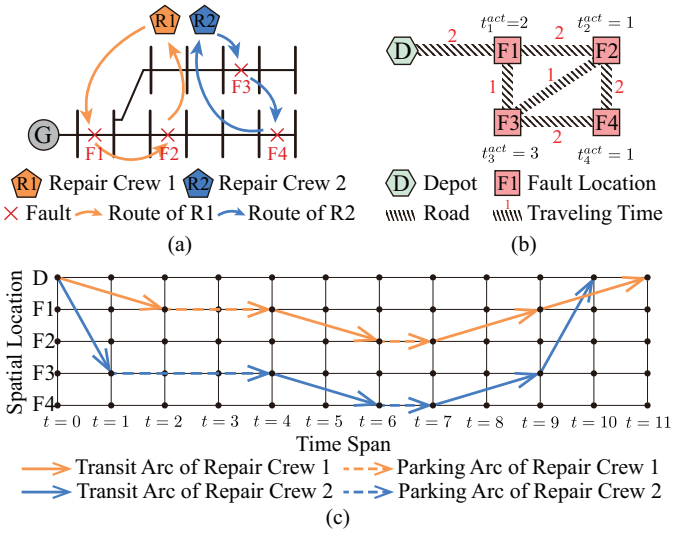

Fig. 2. (a) Distribution system topology and repair crew routing schemes. (b) Spatial location information and actual repair time of damaged components. (c) Time-space network model of repair crews.

where $E_{e,ini}$ is the initial state of charge of the energy storage device e. Constraints (15)-(16) are constraints modeling the operation of energy storages. Active power exchange constraint is modelled in (15). Constraint (16) simulates the evolution of state of charge of an energy storage device. An auxiliary function $f_e(P^{ES}_{e,v,s})$ is introduced in (17) to depict the single dispatch interval relationship between power output and state of charge of an energy storage device.

$$f_e(P^{ES}_{e,v,s}) = \begin{cases} P^{ES}_{e,v,s}\eta^{ch}_e, & \text{if } P^{ES}_{e,v,s} \le 0; \\ P^{ES}_{e,v,s}/\eta^{dch}_e, & \text{if } P^{ES}_{e,v,s} > 0. \end{cases} \tag{17}$$

B. Modeling of Repair Crews

Unlike previous research aiming at fixed repair time and fixed number of stuffs in each repair crews, with the uncertain repair time of fault components taken into consideration in this paper, the number of repair crews as well as the staffs in each repair crew should be adjustable. Thus, we proposed an improved method to repair crew dispatch modeling on the basis of time-space network theory [31]–[34].

As shown in Fig. 2(a), altogether four line outages are identified in the 12-bus distribution system, two repair crews for transmission line maintenance are dispatchable. The available travelling path and travelling time are shown in Fig. 2(b), with certain repair times t_1^{act}, t_2^{act}, t_3^{act} and t_4^{act}. Herein we use the deterministic example to illustrate the basic theory of time-space network model. For the sake of clarity, the uncertainty of repair workloads is not considered here. The modeling of uncertainty of repair workloads in presented in Section II in detail, and the solution method disposing the uncertainty is proposed in Section IV-B.

Fig. 2(c) is the time-space network model of the dispatch schemes shown in Fig. 2(a). The transit arc depicts the travelling process of repair crews while the parking arc denotes the repairing process. The travelling arc is constrained by the availability of traffic path which is shown in Fig. 2(b) and the length of parking arc is held by the degree of damage which is obtained by fast detection of the fault component. The whole process of infrastructure maintenance of each repair crew is captured by a sequence of arcs.

1) Routing Constraints of Time-Space Network:

$$\sum_{(m,u)\in\Omega} \delta^t_{c,(m,u),s} = 1 \quad \forall c \in \mathcal{C}, \forall s \in \mathcal{S}, \forall t \tag{18}$$

$$\sum_{(m,u)\in\Omega^+_m} \delta^t_{c,(m,u),s} = \sum_{(m,u)\in\Omega^-_m} \delta^{t+1}_{c,(m,u),s} \quad \forall c \in \mathcal{C}, \forall s \in \mathcal{S}, \forall t \ne |\mathcal{T}| \tag{19}$$

$$\sum_{(m,u)\in\Omega^+_m} \delta^1_{c,(m,u),s} = \delta^0_{c,(-,m)} \quad \forall c \in \mathcal{C}, \forall m \in \mathcal{N}, \forall s \in \mathcal{S} \tag{20}$$

$$\delta^t_{c,(m,u),s} + \delta^{t+1}_{c,(u,m),s} \le 1 \quad \forall c \in \mathcal{C}, \forall (m,u) \in \Omega, m \ne u, \forall s \in \mathcal{S} \tag{21}$$

where $\delta^t_{c,(m,u),s}$ represents the stare of each repair crew, which values 1 when repair crew c is on the arc from location m to location u at dispatch interval t, and values 0 otherwise. Note that (m,u) is able to denote the arcs shown in Fig. 2(c). It refers to a travelling arc when $m \ne u$, and a parking arc when $m = u$. $\delta^0_{c,(-,m)}$ denote the initial location of each repair crews, which values 1 if repair crew c initially located at locaiton m, and values 0 otherwise. Constraints (18)-(21) are routing constraints of the time-space network model. Constraint (18) is the repair crew state constraint, which ensures each repair crew to be either in a travelling arc or a parking arc, corresponding to either travelling state or repairing state. Constraints (19)-(20) formulate the flow conservation for each repair crew, of which (20) indicates the initial location of each repair crew. Constraint (21) prevents the repair crew from moving directly back to the previous location.

2) Grouping Constraints of Repair Crews:

$$\sum_{c\in\mathcal{C}} \sum_{(m,u)\in\Omega} n^t_{c,(m,u),s} = NR \quad \forall s \in \mathcal{S}, \forall t \tag{22}$$

$$\delta^t_{c,(m,u),s}\underline{n}_c \le n^t_{c,(m,u),s} \le \delta^t_{c,(m,u),s}\overline{n}_c \quad \forall c \in \mathcal{C}, \forall (m,u) \in \Omega, \forall s \in \mathcal{S}, \forall t \tag{23}$$

$$\sum_{c\in\mathcal{C}} \sum_{(m,u)\in\Omega^+_m} n^t_{c,(m,u),s} = \sum_{c\in\mathcal{C}} \sum_{(m,u)\in\Omega^-_m} n^{t+1}_{c,(m,u),s} \quad \forall m \in \mathcal{N}, \forall s \in \mathcal{S}, \forall t \ne |\mathcal{T}| \tag{24}$$

$$\sum_{c\in\mathcal{C}} \sum_{(m,u)\in\Omega^+_m} n^1_{c,(m,u),s} = \sum_{c\in\mathcal{C}} n^0_{c,(-,m)} \quad \forall m \in \mathcal{N}, \forall s \in \mathcal{S} \tag{25}$$

where constraint (22)-(25) formulate the grouping constraints of repair crews. Constraint (22) ensures the conservation of the total number of staffs, while constraint (23) limits the number of staffs in each repair crew, probably due to the capacity of transportation facility. It is worth noting that constraint (23) limit $n^t_{c,(m,u),s}$ to 0 when $\delta^t_{c,(m,u),s}$ is 0. Constraints (24)-(25) compose the flow conservation of each time-space node, of which equation (25) indicates the initial composition of each repair crew.

*Remark 1:*Dynamic crew grouping is allowed by grouping constraints (22)-(25), that is, when multiple repair crews are at the same location at the same time, the staffs regrouping is allowed.

Dynamic crew grouping adjustment is the key idea of crew dispatch dealing with the uncertainties in repair workloads, which effectively boosts the restoration speed of the distribution system. This effect is detailly simulated and analyzed in Section V-A.

C. Modeling of Infrastructure Restoration

As aforementioned, the maintenance work of fault components is modeled by the parking arc. Thus, the status of the fault component is directly related to the length of parking arc and the number of staffs in the repair crew, viz, the cumulative workload.

$$w_{h,t,s} = w_{h,t-1,s} + \Delta T \sum_{c\in\mathcal{C}} n^t_{c,(m,u),s} \quad \forall h \in \mathcal{H}, \forall s \in \mathcal{S}, \forall t \neq 0 \tag{26}$$

$$u_{h,t,s} \leq 1 + (w_{h,t,s} - W^{act}_h)/W^{act}_h \quad \forall h \in \mathcal{H}, \forall s \in \mathcal{S}, \forall t \tag{27}$$

where $w_{h,t,s}$ is the cumulated repair workload of fault component h. Constraint (26)-(27) are coupling constraints of cumulative repair workload and the restoration status of the fault components. In (26), the workload is cumulated by the length of parking arc at location m for maintenance of fault component h and the number of staffs in the repair crew c. Constraint (27) shows that once the cumulated repair workload has exceeded the actual repair workload required by the fault component, viz, the fault component is repaired, the status of fault component $u_{h,t,s}$ is able to be 1, representing that the component is able to be back into operation.

D. Restoration Objective

$$\min \sum_{s\in\mathcal{S}} \alpha_s [\sum_t \sum_{d\in\mathcal{D}} C^D_d (P^D_d - P^R_{d,t,s})\Delta T + \sum_t \sum_{g\in\mathcal{G}} C^G_g P^G_{g,t,s} \Delta T + \sum_t \sum_{c\in\mathcal{C}} C^{RC}_c \sum_{(m,u)\in\Omega} n^t_{c,(m,u),s}] \tag{28}$$

where the first term is the power supply interruption cost, the second term represents the distribution system generation cost, and the third term refers to the routing cost of repair crews. C^D_d, C^G_g and C^{RC}_c denotes the per unit interruption cost, generation cost and transportation cost respectively. Function (28) is the objective function of the post-disaster restoration process.

IV. Implicit Decision Rule Based Solution Method

A. Model Analysis

The optimal restoration model of high renewable penetrated distribution system with the consideration of uncertain repair workload is proposed in Section III, as (2)-(28). The

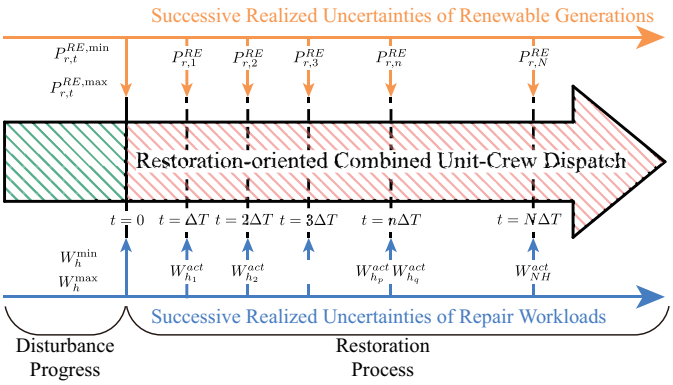

Fig. 3. An illustration of multi-stage decision-making process with successive realized uncertainties.

stochastic characteristic and limited information of renewable generation and repair time make the proposed model a multi-stage stochastic programming problem with nonanticipativity constraints, which is not able to be solved by off-shelf solvers [5], [23], [25]. Moreover, towards providing a safe and fast restoration process, whether renewable energy generation is fully utilized is a tricky question. It improves the restoration speed and reduce the restoration cost, but proposes challenges in restoration dispatch, which is not able to be achieved by deterministic programming method or simple scenario-based stochastic programming method.

Of all the information used in the optimal restoration model, it can be categorized into two groups. The first group contains the uncertain intervals of renewable energy generations and the repair workloads, viz, $W^{\max}_h$, $W^{\min}_h$, $P^{RE,\max}_{r,t}$ and $P^{RE,\min}_{r,t}$, which are deterministic and able to be obtained at the beginning of the restoration process. Another group entails the successively realized uncertainties in observation, viz, the actual renewable energy generations $P^{RE}_{r,t}$ and the actual repair workloads W^{act}_h. Thus, the multi-stage decision-making process of restoration is shown in Fig. 3.

The complete decision-making process includes sequential restoration-oriented combined unit-crew dispatch (RCUCD) decisions made at successive intervals. RCUCD at each dispatch interval optimizes conventional generation outputs, accommodated renewable generations, energy storage power exchanges, restored load consumptions, repair crew routing decisions and grouping decisions.

B. Implicit Decision Rule Based RCUCD Formulation

The implicit decision rule based RCUCD formulation is presented in this section. As aforementioned, RCUCD is a multi-stage stochastic programming problem. The exact solution is hard to derive from its original formulation. Thus, this section introduces the implicit decision rule based reformulation method. The newly formed problem is equal to the original version, and provides the same solution, as proved in [23], [25]. A reduction in the selected scenario set and newly introduced nonanticipativity and real-time dispatch constraints are formulated.

1) All-Scenario-Feasibility in Scenario Selection: As proved in [25], it is essential to select special scenarios for providing robustness to successive dispatch solution. Thus, the scenarios are categorized into two divisions, namely base scenarios and selective vertex scenarios. Moreover, base scenarios are selected for economic consideration, while selective vertex scenarios are for providing a full representation of the uncertainty set, viz, for all-scenario-feasibility in the whole restoration process. In this paper, the base scenario is selected as the expected values of outputs of renewable generations and expected values of repair workloads, as shown in (29).

$$W_{h,s} = \mathbb{E}(W_h), P^{RE}_{r,t,s} = \mathbb{E}(P^{RE}_{r,t}) \quad \forall s \in \hat{\mathcal{S}}^{BS} \tag{29}$$

The selective vertex scenarios are carefully selected from the uncertainty set (1) and (8) to guarantee the all-scenario-feasibility. For example, consider a two bus system with a renewable generation unit at bus 1 and a thermal generation unit at bus 2. The transmission line between bus 1 and 2 requires repair work. In this case, the selective vertex scenarios are formulated as:

$$\hat{\mathcal{S}}^{SVS} = \{(P^{RE,\max}, W^{\max}), (P^{RE,\max}, W^{\min}), (P^{RE,\min}, W^{\max}), (P^{RE,\min}, W^{\min})\} \tag{30}$$

For more details on selective vertex scenarios selection procedure, please refer to [4] and [22]. The newly formed scenario set is represented by $\hat{\mathcal{S}}$.

$$\hat{\mathcal{S}} = \hat{\mathcal{S}}^{BS} \cup \hat{\mathcal{S}}^{SVS} \tag{31}$$

2) Nonanticipativity Constraints in Implicit Decision Rule: The robustness and feasibility for subsequent RCUCD is ensured by the implicit decision rule based method. By introducing safety dispatch region in distributed generation outputs, energy storage state of charge, restored load consumptions, and repair crew grouping decisions, an all-scenario-feasible RCUCD formulation with the nonanticipativity of uncertainties is presented.

The individual power output constraints of distributed generation units (11)-(14) are reformulated as (32)-(37) by introducing the safety output region $[P^{G,\min}_{g,t}, P^{G,\max}_{g,t}]$ and $[Q^{G,\min}_{g,t}, Q^{G,\max}_{g,t}]$.

$$\underline{P}^G_g \le P^{G,\min}_{g,t} \le P^G_{g,t,\hat{s}} \le P^{G,\max}_{g,t} \le \overline{P}^G_g \quad \forall g \in \mathcal{G}, \forall \hat{s} \in \hat{\mathcal{S}}, \forall t \tag{32}$$

$$\underline{Q}^G_g \le Q^{G,\min}_{g,t} \le Q^G_{g,t,\hat{s}} \le Q^{G,\max}_{g,t} \le \overline{Q}^G_g \quad \forall g \in \mathcal{G}, \forall \hat{s} \in \hat{\mathcal{S}}, \forall t \tag{33}$$

$$P^{G,\max}_{g,t} - P^{G,\min}_{g,t-1} \le \Delta^P_g \quad \forall g \in \mathcal{G}, \forall t \tag{34}$$

$$P^{G,\max}_{g,t-1} - P^{G,\min}_{g,t} \le \Delta^P_g \quad \forall g \in \mathcal{G}, \forall t \tag{35}$$

$$Q^{G,\max}_{g,t} - Q^{G,\min}_{g,t-1} \le \Delta^Q_g \quad \forall g \in \mathcal{G}, \forall t \tag{36}$$

$$Q^{G,\max}_{g,t-1} - Q^{G,\min}_{g,t} \le \Delta^Q_g \quad \forall g \in \mathcal{G}, \forall t \tag{37}$$

The safety charging region of the energy storage $[E^{\min}_{e,t}, E^{\max}_{e,t}]$ is derived as (38)-(41).

$$\underline{E}_{e,t} \le E^{\min}_{e,t} \le E_{e,t,\hat{s}} \le E^{\max}_{e,t} \le \overline{E}_{e,t} \quad \forall e \in \mathcal{E}, \forall \hat{s} \in \hat{\mathcal{S}}, \forall t \tag{38}$$

$$-\overline{P}^{ES,ch}_e \le f^{-1}_e(E_{e,t-1,\hat{s}} - E_{e,t,\hat{s}}) \le \overline{P}^{ES,ch}_e \quad \forall e \in \mathcal{E}, \forall \hat{s} \in \hat{\mathcal{S}}, \forall t \tag{39}$$

$$-\overline{P}^{ES,ch}_e \le f^{-1}_e(E^{\max}_{e,t-1} - E^{\min}_{e,t}) \le \overline{P}^{ES,dch}_e \quad \forall e \in \mathcal{E}, \forall t \tag{40}$$

$$-\overline{P}^{ES,ch}_e \le f^{-1}_e(E^{\min}_{e,t-1} - E^{\max}_{e,t}) \le \overline{P}^{ES,ch}_e \quad \forall e \in \mathcal{E}, \forall t \tag{41}$$

The safety load pickup region is formulated as (42)-(43).

$$0 \le P^{R,\min}_{d,t} \le P^R_{d,t,\hat{s}} \le P^{R,\max}_{d,t} \le P^D_d \quad \forall d \in \mathcal{D}, \forall \hat{s} \in \hat{\mathcal{S}}, \forall t \tag{42}$$

$$Q^R_{d,t,\hat{s}} = P^R_{d,t,\hat{s}} \tan(\cos^{-1}\varphi_d) \quad \forall d \in \mathcal{D}, \forall \hat{s} \in \hat{\mathcal{S}}, \forall t \tag{43}$$

The repair crew grouping constraint (23) is transformed into (44).

$$\delta^t_{c,(m,u)}\underline{n}_c \le n^{t,\min}_{c,(m,u)} \le n^t_{c,(m,u),\hat{s}} \le n^{t,\max}_{c,(m,u)} \le \delta^t_{c,(m,u)}\overline{n}_c \quad \forall c \in \mathcal{C}, \forall (m,u) \in \Omega, \forall \hat{s} \in \hat{\mathcal{S}}, \forall t \tag{44}$$

3) Real-Time Dispatch Constraints in Implicit Decision Rule: As for the real-time dispatch problem for current dispatch interval, the dispatch decision depends on the realized uncertainties, including current dispatch interval and previous dispatch intervals. Thus, a shrink on the scenario set at time t is observed, and the real-time dispatch constraints for (32)-(33), (38), (42), (44) are formulated as below.

$$P^{G,\min *}_{g,t} \le P^G_{g,t} \le P^{G,\max *}_{g,t} \quad \forall g \in \mathcal{G} \tag{45}$$

$$Q^{G,\min *}_{g,t} \le Q^G_{g,t} \le Q^{G,\max *}_{g,t} \quad \forall g \in \mathcal{G} \tag{46}$$

$$E^{\min *}_{e,t} \le E_{e,t} \le E^{\max *}_{e,t} \quad \forall e \in \mathcal{E} \tag{47}$$

$$P^{R,\min *}_{d,t} \le P^R_{d,t} \le P^{R,\max *}_{d,t} \quad \forall d \in \mathcal{D} \tag{48}$$

$$n^{t,\min *}_{c,(m,u)} \le n^t_{c,(m,u)} \le n^{t,\max *}_{c,(m,u)} \quad \forall c \in \mathcal{C}, \forall (m,u) \in \Omega \tag{49}$$

For multi-interval related constraints (34)-(37), (39)-(41), the update rule is to replace the safety operation region variables of dispatch interval $t-1$ by the actual dispatch scheme. For example, the safety operation region variables $P^{G,\min}_{g,t-1}$ and $P^{G,\max}_{g,t-1}$ are both replaced by the realization of power output $P^G_{g,t-1}$. The newly formulated real-time dispatch constraints are not shown here due to space reason.

4) Full Implicit Decision Rule Based RCUCD Formulation: Considering the selected scenario set $\hat{\mathcal{S}}$, the original restoration objective function (28) is then transformed to (50), where $\alpha_{\hat{s}}$ is the weighting factor of each scenario. Thus, the full implicit decision rule based RCUCD (F-RCUCD) model for dispatch interval $n\Delta T$ is formulated as:

$$\min \sum_{\hat{s}\in\hat{\mathcal{S}}} \alpha_{\hat{s}} [\sum_{t \ge n\Delta T} \sum_{d \in \mathcal{D}} C^D_d (P^D_d - P^R_{d,t,\hat{s}}) \Delta T + \sum_{t \ge n\Delta T} \sum_{g \in \mathcal{G}} C^G_g P^G_{g,t,\hat{s}} \Delta T + \sum_{t \ge n\Delta T} \sum_{c \in \mathcal{C}} C^{RC}_c \sum_{(m,u)\in\Omega} n^t_{c,(m,u),\hat{s}}] \tag{50}$$

$$\text{s.t. (2)-(8),(18)-(22),(24)-(27)} \tag{51}$$

TABLE I
INFORMATION AND DECISION VARIABLES IN F-RCUCD

Constraints	Known Information	Decision Variables
Nonanticipativity constraints (29)-(41)	$W_h^{\max}$, $W_h^{\min}$, $P_{r,t}^{RE,\max}$, $P_{r,t}^{RE,\min}$.	$P_{g,t}^{G,\min}$, $P_{g,t}^{G,\max}$, $Q_{g,t}^{G,\min}$, $Q_{g,t}^{G,\max}$, $E_{e,t}^{\min}$, $E_{e,t}^{\max}$, $P_{d,t}^{R,\min}$, $P_{d,t}^{R,\max}$, $n_{c,(m,u)}^{t,\min}$, $n_{c,(m,u)}^{t,\max}$.
Real-time dispatch constraints (47)-(51)	W_h^{act}, $P_{r,t}^{RE}$, and dispatch results of the previous dispatch interval.	$P_{g,t}^{G}$, $Q_{g,t}^{G}$, $E_{e,t}$, $P_{d,t}^{R}$, $\delta_{c,(m,u)}^{t}$, $n_{c,(m,u)}^{t}$.

$$\text{(29)-(34),(35)-(40)} \quad \forall t > n\Delta T \tag{52}$$

$$\text{real-time dispatch constraints} \quad t = n\Delta T \tag{53}$$

Note that nonanticipativity and all-scenario-feasibility of full implicit decision rule based RCUCD (F-RCUCD) is independent to the value of weighting factor, as long as the scenario set $\hat{\mathcal{S}}$ is selected as stated in subsection *1)*. The known information and decision variables in the F-RCUCD is presented in Tab. I.

The full implicit decision rule based RCUCD (F-RCUCD) is formulated as a mixed integer linear programming (MILP) problem, which can be solved by off-the-shelf solvers. The F-RCUCD is a multi-interval optimization problem which need to be solved in successive dispatch intervals in a rolling way. This could be a computational burden for large scale distribution systems, especially for complex urban distribution systems. Thus, a simplification implicit decision rule based formulation of RCUCD (S-RCUCD) is presented in the next subsection.

C. Simplified implicit decision rule based RCUCD Formulation

All safety operation regions optimized by F-RCUCD at all dispatch intervals are able to provide nonanticipativity and all-scenario-feasibility. Thus, to reduce the computational burden, we decide to find equilibrium point of the trade-off between economic and computational complexity. A simplified implicit decision rule based RCUCD, named S-RCUCD is proposed. At the beginning of the restoration process, F-RCUCD for safety operation region problem (50)-(52) considering all intervals is solved. Note that by the transformation of (50) to single interval and with constraints (51) and (53), the computational burden can be released. Moreover, by updating the safety operation region in every dispatch interval according to the look-ahead implicit decision rule based RCUCD for several future intervals, it formulates the rolling look-ahead RCUCD (R-RCUCD).

Considering that the F-RCUCD brings heavy computational burden to distribution system operators, the computational efficiency and effectiveness of conventional restoration dispatch method, S-RCUCD and R-RCUCD will be fully compared and detailly analyzed in the numerical tests.

V. NUMERICAL TESTS

In this section, numerical tests are arranged on modified IEEE 34-bus [35] and 69-bus [36] distribution systems. All simulations are implemented via MATLAB R2020a platform with GUROBI 9.0.2, on an Intel(R) Core(TM) i7-10510U CPU @1.80GHz laptop with 16 GB RAM.

TABLE II
UNCERTAIN WORKLOAD INTERVALS OF DAMAGED COMPONENTS

Damaged Component	Location	Uncertain Workload Intervals	Actual Workloads
F1	802-806	[4,8] *man-hours*	4 *man-hours*
F2	814-850	[2,4] *man-hours*	4 *man-hours*
F3	830-854	[4,12] *man-hours*	10 *man-hours*
F4	832-888	[4,8] *man-hours*	6 *man-hours*
F5	824-828	[4,8] *man-hours*	7 *man-hours*
F6	842-844	[2,4] *man-hours*	2 *man-hours*
F7	836-862	[4,8] *man-hours*	8 *man-hours*

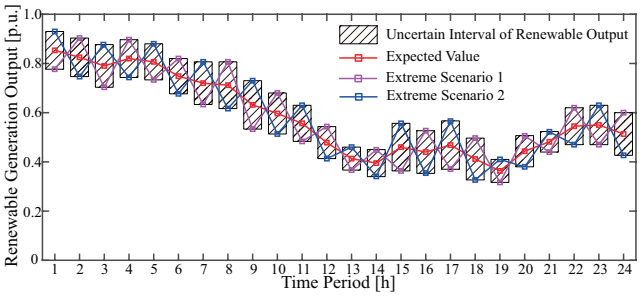

Fig. 4. The 24-hour cycle period of renewable energy generations.

A. Modified IEEE 34-Bus Distribution System Case Study

1) Basic System Information: The modified IEEE 34-bus distribution system contains 33 transmission lines, 3 conventional generation units at bus 800, 840, 856 and 4 renewable energy generation units at bus 810, 822, 846, 864. The capacity of distribution generation units is 400 kW, whereas the capacity of renewable energy generation is 300 kW. The topology of the test system is shown in Fig. 8. The renewable energy penetration rate is 50%. The generation cost of conventional generation units is \$0.5/kWh [31], [32]. The load is categorized into high and low priority, with the interruption cost of \$10/kWh and \$5/kWh [33]. Altogether 7 line outages are detected after the disaster. The uncertainty intervals of repair workloads corresponding to F1 to F7 which are known initially are presented in Tab. II. The actual workload which will be known after a repair crew reach the location is in the last column. Information of uncertainties in renewable energy generation is shown in Fig. 4. The assumption is made that all distributed renewable generation units follow the same output uncertain interval but with different random realized values.

Note that a 24-hour cycle period in renewable energy generation [23] is assumed for the sake of simplicity. For detailed load data, refer to [35], and the modification is done by aggregating the distributed load to the start bus of the transmission line. Altogether 12 staffs, 3 repair crews, and 1 depot is taken into consideration, while the lower and upper boundary of capacity limitation on each crew is 2 and 6, respectively. Spatial locations of line outages are depicted in Fig. 5 with the travelling time data. Routing cost per unit length is set as \$50 [31]. The case study is implemented as below.

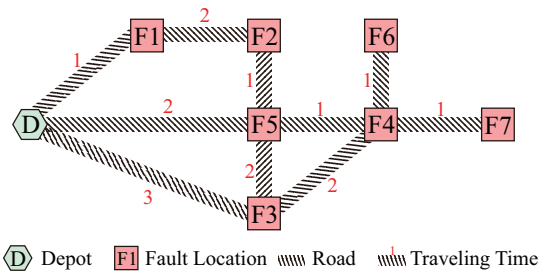

Fig. 5. Spatial location of 7 line outages in the distribution system with travelling time data.

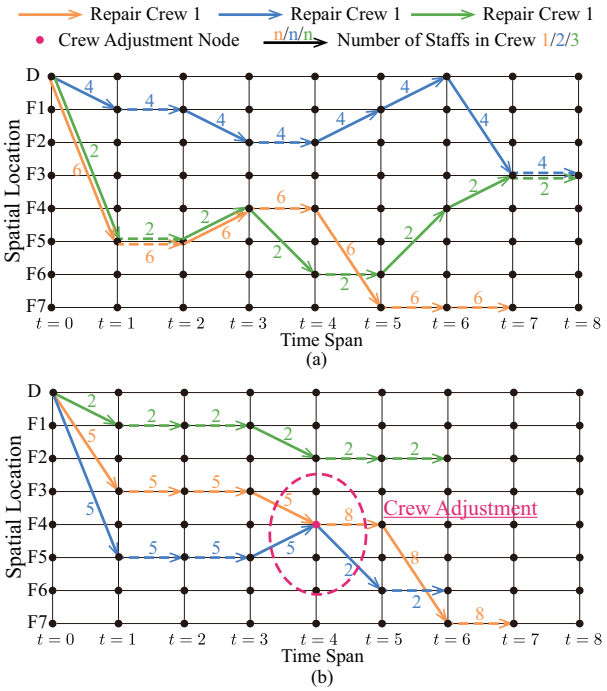

Fig. 6. Comparison on routing and grouping decisions. (a) Routing and grouping decisions of Case 1. (b) Routing and grouping decisions of Case 2. Note that these two subplots focus on the routing decisions before complete system infrastructure restoration.

2) Infrastructure Restoration Analysis: We consider a separated repair crew dispatch problem in this part, and the cases are set as below.

Case 1: ignore the real distance between locations (set the distance between every two of the locations as a one-hour trip), and the dynamic crew grouping strategies are prohibited.

Case 2: ignore the real distance between locations and the dynamic crew grouping strategies are allowed.

Case 3: utilize the real distance between locations and the dynamic crew grouping strategies are prohibited.

Case 4: utilize the real distance between locations and the dynamic crew grouping strategies are allowed.

From the comparison of simulation results between Case 1 and Case 2, the differences of enabling dynamic crew grouping is shown in Fig. 6. The number on arcs denote the number of staffs in each repair crew. Note that all crews should route back to the depot. However, due to space reason, the time-space network illustrations focus on the routing and grouping decision before all fault components are restored. It is clearly illustrated that a dynamic repair crew adjustment between repair crew 1 and repair crew 2 was observed at 4:00 AM in Fig. 6(b). 3 staffs from repair crew 2 joined repair crew 1 for dealing with the large repair workload at F4. This behavior in real-time dispatch is intuitive and understandable. At 4:00 AM, repair crew 1 and 2 arrived at fault component F4 at the same time. After a fast detection, it is found that the actual required repair work load for F4 is relatively high, in other words, F4 is seriously damaged. Thus, for a faster restoration for the distribution system, dynamic grouping behavior took place. Thus, a regrouping result as crew 1 with 8 staffs and crew 2 with 2 staffs is shown. Positive results appear with this dynamic grouping behavior. In Case 1, the total infrastructure restoration time is 8 hours, while it only costs 7 hours in Case 2. An efficiency improvement of 12.5% is observed. Considering that this is a result of a specific realization, it is promising that in dealing with the uncertainties in repair workloads, dynamic crew grouping is effective in boosting the speed of infrastructure restoration.

TABLE III
INFRASTRUCTURE RESTORATION TIME OF CASES

Case	Cumulated Travelling Time	Cumulated Repair Time	Restoration Time
1	13h	10h	8h
2	8h	11h	7h
Δ_{12}	5h	-1h	12.50%
3	39h	11h	17h
4	29h	12h	14h
Δ_{34}	10h	-1h	17.65%

The infrastructure restoration time of all cases are shown in Tab. III. The indices cumulated travelling time and cumulated repair time are introduced to depict the effectiveness of implicit decision rule based dynamic crew grouping dispatch method.

$$T^{CT} = \sum_{t} \sum_{c \in \mathcal{C}} \sum_{m \neq u} \delta^{t}_{c,(m,u)} \tag{54}$$

$$T^{CR} = \sum_{t} \sum_{c \in \mathcal{C}} \sum_{m = u} \delta^{t}_{c,(m,u)} \tag{55}$$

where T^{CT} and T^{CR} denote the cumulated travelling time and the cumulated repair time, respectively.

Along with the comparison of altogether 4 cases, we can see that the dynamic crew grouping behaviors do not affect the cumulated repair time a lot, while greatly influencing the cumulated travelling time of the whole infrastructure restoration process. The dynamic crew grouping makes a great reduction on the travelling time. In comparison between Case 1 and Case 2, the cumulated travelling time reduced by 5 hours. Moreover, in comparison between Case 3 and Case 4, the cumulated travelling time reduced by 10 hours. This overcomes the slight increment in cumulated repair time (1 hour in both cases, which could be ignored in larger cases), which finally results in the efficiency improvement of infrastructure restoration by 12.50% and 17.65%.From the comparison between the improvements on Case 1 and Case 3, the travelling time reduction effect is more significant if the

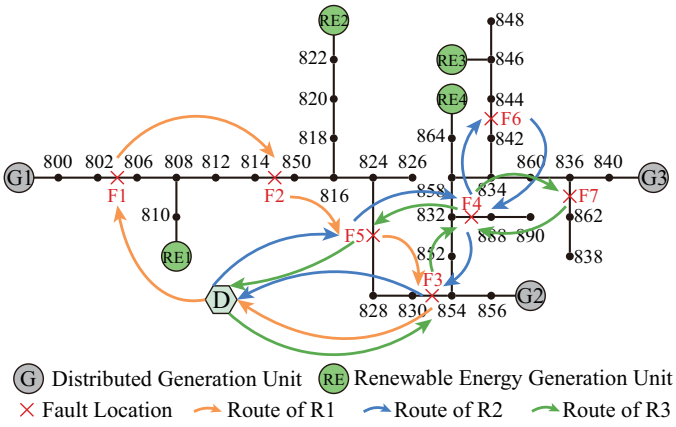

Fig. 7. Restoration process of Case 1 for the expected scenario.

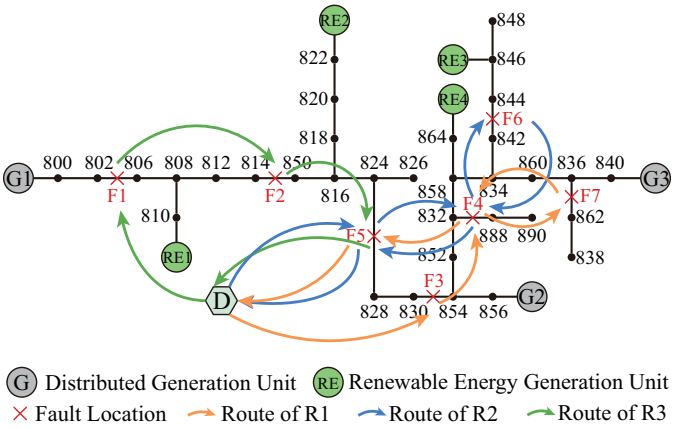

Fig. 8. Restoration process of Case 2 and Case 3 for the expected scenario.

distance between fault components is longer. For the real-lift urban distribution power system, it is common that the system covers a large area and fault components locate sparsely. Under this situation, the proposed dynamic grouping method will certainly enhance the infrastructure efficiency at a higher level.

3) Load Service Restoration Analysis: To show the effectiveness of the implicit decision rule based RCUCD method in the distribution system service restoration, we developed three cases as below. Note that all cases include the real distance between locations.

Case 1: original RCUCD model (2)-(28), formulated as a single-stage stochastic programming problem (the decision-making process is omitted, which is common in other literatures) with randomly generated 10 scenarios. Note that the nonanticipativity is not considered in this case.

Case 2: implicit decision rule based simplified RCUCD formulation (S-RCUCD), with one all-interval safety operation region problem (50)-(53) and successive real-time simplified dispatch problem for each dispatch interval based on the resulted safety operation regions.

Case 3: implicit decision rule based simplified RCUCD model with rolling look-ahead multi-interval safety operation region problem (50)-(53) and successive real-time simplified RCUCD based on the rolling updated look-ahead safety operation regions, that is, R-RCUCD. To balance the economic and complexity, the rolling and look-ahead dispatch period is set as 3 intervals.

The three dispatch methods and their corresponding commitment solutions are tested by the two selected extreme scenarios shown in Fig. 4, namely extreme scenario 1 and extreme scenario 2, along with eight randomly generated scenarios (including renewable energy generation and repair workload). The mean restoration results of altogether 10 scenarios are shown in Tab. IV.

According to the row named rate of renewable energy accommodation, it is obvious that Case 2 and Case 3 are able to provide a full accommodation dispatch scheme, whereas the Case 1 can only utilize 63.48% of the renewable energy generation. As aforementioned, in a distribution system with high penetration of renewable energy, utilization of renewable energy is supportive to post-disaster restoration. As we can see, in the comparison between Case 1 and Case 2, an 8-hour advance is observed for the time of 80% load restoration. This is partly due to the full utilization of renewable energy generation in Case 2. This proved the importance of renewable energy utilization in high renewable penetrated distribution systems.

TABLE IV
RESTORATION RESULT OF THREE RESTORATION SCHEMES

Case	1	2	3
Rate of Renewable Energy Accommodation	63.48%	100.00%	100.00%
Time of 80% Restoration*	18h	10h	10h
Time of 100% Restoration*	25h	14h	14h
Power Supply Interruption Cost	$13263.59	$9684.40	$9164.32
Generation Cost	$6309.37	$5408.61	$4942.09
Routing Cost	$2550	$2050	$1950
Total Cost	$22122.96	$17107.01	$16056.41

* Note that 80% of restoration considers the load service only, while 100% of restoration considers both load service and system infrastructure.

The routing efficiency of repair crews is also able to be observed in Tab. III, and the routing decision is presented in Fig. 7 and 8. According to the time of 100% restoration, it always depends on the infrastructure recovery time, which is largely influenced by repair crews routing and grouping. A 11-hour advance in fully restoration between Case 1 and Case 2 is presented. Moreover, the comparison on routing costs directly illustrates the effectiveness of implicit decision rule based simplified RCUCD method, for that a 19.61% and a 23.53% of cost reduction is shown in Case 2 and Case 3.

Considering that the effectiveness of the proposed S-RCUCD method in renewable energy accommodation and repair crews routing, the reduction in total cost of restoration process is reasonable. Compared with the cost of Case 1, the proposed method achieved a 22.67% reduction. Further, a 6.14% cost reduction is observed in the comparison between Case 2 and Case 3. This illustrates the advantage of the rolling look-ahead RCUCD (R-RCUCD) over single-interval simplified RCUCD method. However, the computation complexity of each dispatch interval increases at the same time. Thus, the choice of rolling single-interval or multi-interval look-ahead RCUCD (R-RCUCD) depends on the scale of distribution system together with the computation capacity of distribution system operator.

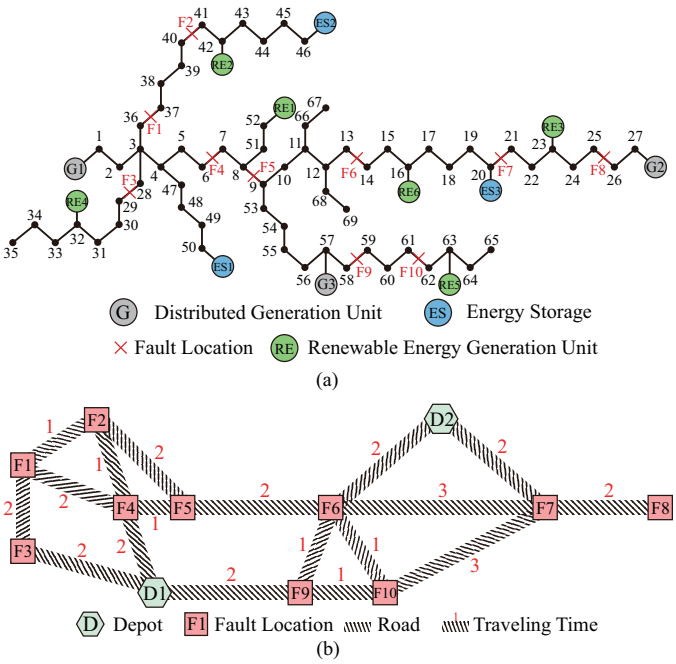

Fig. 9. Basic system information of modified IEEE 69 bus distribution system.

B. Modified IEEE 69-Bus Distribution System Case Study

1) Basic System Information: The modified IEEE 69-bus distribution system contains 68 transmission lines, 3 distributed generation units, 6 renewable energy generation units, and 3 energy storages. The locations are shown in Fig. 9. The total load of the distribution system is 3802.19 kW and 2694.60 kVar. The capacity of each distributed generation unit is 800 kW, and the capacity of each renewable energy generation unit is 600 kW. The renewable penetration rate in this distribution system is 60%. The capacity of each energy storage is 400 kW with the original state of charge as 60%. The cost information is the same as the modified IEEE 34-bus distribution system case study. Altogether 10 line outages occur in the disaster, each of them has an uncertain repair workload from 4 to 8 man-hours, and their realizations are all set to 6 man-hours. Two depots are set up and each contains 20 staffs for 3 repair crews.

2) Computational Complexity Analysis: Considering that the immediate restoration is critical in post-disaster period, we focus on the first 24-hour period of restoration. Three same cases of load service restoration analysis in IEEE 34-distribution system case study are set up.

It is shown clearly in Tab. V, for a conventional programming restoration method (Case 1), its total computation time is 138.9s, while the restoration result is 64.74% of load service is restored in the first 24-hour period, which is lower than the result of proposed method. The lower restoration efficiency is caused by the ignorance of nonanticipativity and all-scenario-feasibility, which directly results in the unavailability in full-renewable-accommodation. Moreover, the trade-off between restoration effect and computation complexity is illustrated by the comparison between Case 2 and Case 3. For real-time dispatch computation, it costs 15.7s for the S-RCUCD in Case 2, while costs 26.1s for the R-RCUCD method in Case 3. Meanwhile, an uplift of 7.52% in restoration result is observed. Thus, from the aforementioned numerical tests, conclusions on computational efficiency and restoration result of all methods mentioned in this paper are drawn. With regard to computational efficiency, there is S-RCUCD (best efficiency) $>$ R-RCUCD $>$ F-RCUCD (relatively low performance in computational efficiency); with regard to restoration effect, there is F-RCUCD (best restoration effect) $>$ R-RCUCD $>$ S-RCUCD (relatively low restoration effect). Therefore, the distribution system operator can choose the above methods according to the computational resources and the scale of distribution system.

TABLE V
COMPUTATIONAL COMPLEXITY ANALYSIS OF PROPOSED METHOD

Case	1	2	3
Restoration Result	64.74%	74.78%	82.30%
Total Computation Time	138.9s	772.3s	1072.8s
Average Computation Time of Real-Time Dispatch*	-	15.7s	26.1s

* Note that the average computation time of real-time dispatch is the average of 24 dispatch intervals. Specifically, the average computation time of real-time dispatch of Case 3 includes the multi-interval look-ahead dispatch for safety operation region solutions.

VI. CONCLUSION

In this paper, we focus on the dispatch decision making process in the restoration of distribution systems with high penetration of renewable energy. A detailed "wait and see" model of repair workload of fault components is proposed to capture the nonanticipativity of repair workloads. Further, a dynamic crew grouping dispatch algorithm based on time-space network is proposed to dispose the uncertainty of workloads. Together with the uncertainty of renewable energy generations, a restoration-oriented combined unit-crew dispatch (RCUCD) model is set up. Based on implicit decision rules, the RCUCD model is reformulated into a mixed integer linear programming (MILP) F-RCUCD problem. Then, to reduce the computational complexity, the simplified RCUCD (S-RCUCD) and rolling look-ahead RCUCD (R-RCUCD) model is proposed. The effectiveness and efficiency of the proposed methods are verified by case studies.

Moreover, we realized that the frequency constraints are critical for distribution systems with high penetration of renewable energy. Therefore, linearization of dynamic frequency regulation and its reformulation in implicit decision rule method is the next research topic.

REFERENCES

[1] I. E. Agency. Net zero by 2050: A roadmap for the global energy sector. [Online]. Available: https://www.iea.org/reports/worldenergy-outlook-2020/achieving-net-zero-emissions-by-2050

[2] Y. Wang, C. Chen, J. Wang, and R. Baldick, "Research on resilience of power systems under natural disasters—a review," *IEEE Trans. Power Syst.*, vol. 31, no. 2, pp. 1604–1613, Mar. 2016, doi: 10.1109/TPWRS.2015.2429656.

[3] R. Rockafellar and R. Wets, *Nonanticipativity and L^1-Martingales in Stochastic Optimization Problems*, mar 2009, vol. 6, pp. 170–187. ISBN 978-3-642-00785-9

[4] I. Evstigneev and S. Flåm, *Stochastic programming: nonanticipativity and lagrange multipliersStochastic Programming: Nonanticipativity and Lagrange Multipliers*, jan 2001, pp. 2506–2512. ISBN 978-0-7923-6932-5

[5] Q. Zhai, X. Li, X. Lei, and X. Guan, "Transmission constrained uc with wind power: An all-scenario-feasible milp formulation with strong nonanticipativity," *IEEE Trans. Power Syst.*, vol. 32, no. 3, pp. 1805–1817, 2017, doi: 10.1109/TPWRS.2016.2592507.

[6] T. Ding, Y. Hu, and Z. Bie, "Multi-stage stochastic programming with nonanticipativity constraints for expansion of combined power and natural gas systems," *IEEE Trans. Power Syst.*, vol. 33, no. 1, pp. 317–328, 2018, doi: 10.1109/TPWRS.2017.2701881.

[7] N. Edirisinghe, "Bound-based approximations in multistage stochasticprogramming: Nonanticipativity aggregation," *Ann. Oper. Res.*, vol. 85, pp. 103–127, 1999.

[8] A. Lorca, X. A. Sun, E. Litvinov, and T. Zheng, "Multistage adaptive robust optimization for the unit commitment problem," *Oper. Res.*, vol. 64, no. 1, pp. 32–51, 2016.

[9] A. Lorca and X. A. Sun, "Multistage robust unit commitment with dynamic uncertainty sets and energy storage," *IEEE Trans. Power Syst.*, vol. 32, no. 3, pp. 1678–1688, 2017, doi: 10.1109/TPWRS.2016.2593422.

[10] Z. Bie, Y. Lin, G. Li, and F. Li, "Battling the extreme: A study on the power system resilience," *Proc. IEEE*, vol. 105, no. 7, pp. 1253–1266, 2017, doi: 10.1109/JPROC.2017.2679040.

[11] M. Panteli, P. Mancarella, D. N. Trakas, E. Kyriakides, and N. D. Hatziargyriou, "Metrics and quantification of operational and infrastructure resilience in power systems," *IEEE Trans. Power Syst.*, vol. 32, no. 6, pp. 4732–4742, 2017, doi: 10.1109/TPWRS.2017.2664141.

[12] M. Panteli, D. N. Trakas, P. Mancarella, and N. D. Hatziargyriou, "Power systems resilience assessment: Hardening and smart operational enhancement strategies," *Proc. IEEE*, vol. 105, no. 7, pp. 1202–1213, 2017, doi: 10.1109/JPROC.2017.2691357.

[13] A. Arif, Z. Wang, J. Wang, and C. Chen, "Power distribution system outage management with co-optimization of repairs, reconfiguration, and dg dispatch," *IEEE Trans. Smart Grid*, vol. 9, no. 5, pp. 4109–4118, 2018, doi: 10.1109/TSG.2017.2650917.

[14] H. Sekhavatmanesh and R. Cherkaoui, "A multi-step reconfiguration model for active distribution network restoration integrating dg start-up sequences," *IEEE Trans. Sust. Energy*, vol. 11, no. 4, pp. 2879–2888, 2020, doi: 10.1109/TSTE.2020.2980890.

[15] Z. Cui, X. Bai, P. Li, B. Li, J. Cheng, X. Su, and Y. Zheng, "Optimal strategies for distribution network reconfiguration considering uncertain wind power," *CSEE J. Power Energy Syst.*, vol. 6, no. 3, pp. 662–671, 2020, doi: 10.17775/CSEEJPES.2018.01410.

[16] B. Chen, Z. Ye, C. Chen, J. Wang, T. Ding, and Z. Bie, "Toward a synthetic model for distribution system restoration and crew dispatch," *IEEE Trans. Power Syst.*, vol. 34, no. 3, pp. 2228–2239, 2019, doi: 10.1109/TPWRS.2018.2885763.

[17] Y. Wang, Y. Xu, J. Li, C. Li, J. He, J. Liu, and Q. Zhang, "Dynamic load restoration considering the interdependencies between power distribution systems and urban transportation systems," *CSEE J. Power Energy Syst.*, vol. 6, no. 4, pp. 772–781, 2020, doi: 10.17775/CSEEJPES.2020.02250.

[18] S. Mousavizadeh, A. Alahyari, S. R. M. Ghodsinya, and M.-R. Haghifam, "Incorporating microgrids coupling with utilization of flexible switching to enhance self-healing ability of electric distribution systems," *Prot. Contr. Modern Power Syst.*, vol. 6, no. 1, p. 24, 2021. [Online]. Available: https://doi.org/10.1186/s41601-021-00197-9

[19] P. Gautam, P. Piya, and R. Karki, "Resilience assessment of distribution systems integrated with distributed energy resources," *IEEE Trans. Sust. Energy*, vol. 12, no. 1, pp. 338–348, 2021, doi: 10.1109/TSTE.2020.2994174.

[20] W. Liu, J. Zhan, C. Y. Chung, and L. Sun, "Availability assessment based case-sensitive power system restoration strategy," *IEEE Trans. Power Syst.*, vol. 35, no. 2, pp. 1432–1445, 2020, doi: 10.1109/TPWRS.2019.2940379.

[21] W. Liu and F. Ding, "Hierarchical distribution system adaptive restoration with diverse distributed energy resources," *IEEE Trans. Sust. Energy*, vol. 12, no. 2, pp. 1347–1359, 2021, doi: 10.1109/TSTE.2020.3044895.

[22] G. Huang, J. Wang, C. Chen, J. Qi, and C. Guo, "Integration of preventive and emergency responses for power grid resilience enhancement," *IEEE Trans. Power Syst.*, vol. 32, no. 6, pp. 4451–4463, 2017, doi: 10.1109/TPWRS.2017.2685640.

[23] Y. Zhou, Q. Zhai, and L. Wu, "Multistage transmission-constrained unit commitment with renewable energy and energy storage: Implicit and explicit decision methods," *IEEE Trans. Sust. Energy*, vol. 12, no. 2, pp. 1032–1043, 2021, doi: 10.1109/TSTE.2020.3031054.

[24] Y. Lin, B. Chen, J. Wang, and Z. Bie, "A combined repair crew dispatch problem for resilient electric and natural gas system considering reconfiguration and dg islanding," *IEEE Trans. Power Syst.*, vol. 34, no. 4, pp. 2755–2767, 2019, doi: 10.1109/TPWRS.2019.2895198.

[25] Y. Zhou, Q. Zhai, M. Zhou, and X. Li, "Generation scheduling of self-generation power plant in enterprise microgrid with wind power and gateway power bound limits," *IEEE Trans. Sust. Energy*, vol. 11, no. 2, pp. 758–770, 2020, doi: 10.1109/TSTE.2019.2905280.

[26] A. Arif, S. Ma, Z. Wang, J. Wang, S. M. Ryan, and C. Chen, "Optimizing service restoration in distribution systems with uncertain repair time and demand," *IEEE Trans. Power Syst.*, vol. 33, no. 6, pp. 6828–6838, 2018, doi: 10.1109/TPWRS.2018.2855102.

[27] C. Chen, J. Wang, and D. Ton, "Modernizing distribution system restoration to achieve grid resiliency against extreme weather events: An integrated solution," *Proc. IEEE*, vol. 105, no. 7, pp. 1267–1288, 2017, doi: 10.1109/JPROC.2017.2684780.

[28] Z. Wang, B. Chen, J. Wang, and C. Chen, "Networked microgrids for self-healing power systems," *IEEE Trans. Smart Grid*, vol. 7, no. 1, pp. 310–319, 2016, doi: 10.1109/TSG.2015.2427513.

[29] H. Farzin, M. Fotuhi-Firuzabad, and M. Moeini-Aghtaie, "Enhancing power system resilience through hierarchical outage management in multi-microgrids," *IEEE Trans. Smart Grid*, vol. 7, no. 6, pp. 2869–2879, 2016, doi: 10.1109/TSG.2016.2558628.

[30] Y. Xu, C.-C. Liu, Z. Wang, K. Mo, K. P. Schneider, F. K. Tuffner, and D. T. Ton, "Dgs for service restoration to critical loads in a secondary network," *IEEE Trans. Smart Grid*, vol. 10, no. 1, pp. 435–447, 2019, doi: 10.1109/TSG.2017.2743158.

[31] S. Yao, P. Wang, and T. Zhao, "Transportable energy storage for more resilient distribution systems with multiple microgrids," *IEEE Trans. Smart Grid*, vol. 10, no. 3, pp. 3331–3341, 2019, doi: 10.1109/TSG.2018.2824820.

[32] X. Liu, C. B. Soh, S. Yao, H. Zhang, and T. Zhao, "Operation management of multiregion battery swapping–charging networks for electrified public transportation systems," *IEEE Trans. Transp. Electrif.*, vol. 6, no. 3, pp. 1013–1025, 2020, doi: 10.1109/TTE.2020.3001400.

[33] S. Yao, P. Wang, X. Liu, H. Zhang, and T. Zhao, "Rolling optimization of mobile energy storage fleets for resilient service restoration," *IEEE Trans. Smart Grid*, vol. 11, no. 2, pp. 1030–1043, 2020, doi: 10.1109/TSG.2019.2930012.

[34] L. Jiang, X. Li, T. Long, R. Zhou, J. Jiang, Z. Bie, H. Tian, G. Li, and Y. Ling, "Resilient service restoration for distribution systems with mobile resources using floyd-based network simplification method: Resilient service restoration for ds with mobile resources using floyd-based network simplification method," *IET Gener. Transm. Distrib.*, vol. 16, no. 3, pp. 414–429, Sep. 2021.

[35] I. P. A. D. F. W. Group. 34-bus feeder. [Online]. Available: http://sites.ieee.org/pes-testfeeders/resources/

[36] M. Baran and F. Wu, "Optimal capacitor placement on radial distribution systems," *IEEE Transactions on Power Delivery*, vol. 4, no. 1, pp. 725–734, 1989, doi: 10.1109/61.19265.